647. FRF based substructuring and decoupling of substructures

Eun-Taik Lee[1], Hee-Chang Eun[2]
[1] School of Architecture & Building Science, Chung-Ang University, Korea
[2] Department of Architectural Engineering,
Kangwon National University, Chuncheon, Korea
E-mail: *heechang@kangwon.ac.kr*

(Received 10 July 2011; accepted 5 September 2011)

Abstract. This study considers FRF (frequency response function) based substructuring and decoupling of substructures for the dynamic analysis of complicated huge structures utilizing compatibility conditions between adjacent substructures. This work includes: 1) the derivation of updated FRF matrix for dynamic system subjected to frequency or time dependent constraints in the frequency-domain, 2) the synthesis and decoupling of subsystems based on the dual domain approach using compatibility conditions between adjacent subsystems, 3) the evaluation of the validity of the proposed methods through numerical applications. It is expected that the proposed methods will be utilized as the basic formulation in investigating the dynamic characteristics of partitioned or synthesized system.

Keywords: FRF, substructuring, decoupling, compatibility, constraint force, dual domain.

1. Introduction

There have been a lot of efforts in the dynamic analysis of complicated huge structures. Substructuring partitions a complicated structure into several substructures and assembles them together by proper process in the satisfaction of compatibility conditions. Conversely, decoupling detaches known substructures from an entire structure and predicts the dynamic characteristics of its unknown residual structure. Such substructuring and decoupling procedures are synthesized and disassembled utilizing compatibility conditions between substructures, respectively. The adjacent substructures are interdependently affected by the coupling forces at contact surface. The coupling forces indicate the constraint forces required for satisfying the compatibility conditions. The substructuring and decoupling of substructure are carried out by the addition and removal of the coupling forces at the interfaces, respectively.

The substructuring and decoupling can be performed in the time-domain and frequency-domain bases. In the time-domain methods each component is described by mass, damping and stiffness matrices, while in the frequency-domain methods – by frequency-dependent data. The coupling forces can be expressed as the functions of time and frequency in the time-domain and frequency-domain, respectively.

The dynamic equation in the frequency-domain of a structure involves FRF matrix as a coefficient matrix to estimate the dynamic characteristics. FRF-based substructuring (FBS) and decoupling (FBD) methods predict the dynamic characteristics of synthesized and decoupled substructures on the basis of FRFs of independent substructures. The analytical process requires the FRF matrix of substructures and the compatibility conditions to combine and partition them. At this time, the total degrees of freedom can retain the interface degrees of freedom of each substructure or not.

Substructure coupling methods are the techniques to reduce the model-order of huge structural systems by synthesizing substructures. Hurty [1] introduced the component mode synthesis (CMS) method in 1960. The method is to combine subdivided substructures into an approximate mathematical model of the full structural system using the displacement

constraints and the interface forces at the interfaces. A number of variants of the methods were proposed and employed [2-7]. De Lima et. al [8] suggested a modeling methodology of structural systems supported by translational and rotational viscoelastic mounts or joints based on a FRF coupling technique. Based on the dual and primal assembly of substructures, Klerk et. al [9] introduced the Lagrange Multiplier Frequency based Substructuring method. The Lagrange Multiplier defines the coupling forces between the adjacent substructures.

The decoupling of structural system is performed to obtain the information of residual system from the known dynamic behavior of the entire system and removed subsystems. As a simple application, the decoupling is performed to get rid of the effect of the accelerometer mass on FRF measurements. The decoupling problem can be seen as the reverse of the substructuring problem in the meaning of removing the coupling forces. Starting from the known dynamic behavior of the entire system and from information about the remaining part of the structural system, D'Ambrogio and Fregolent [10] identified the dynamic behavior of a structural subsystem. They provided the dual domain decomposition method by the deletion of a prescribed substructure so that it is the negative role.

Allen et. al [11] presented a method that removes the effects of a flexible fixture from an experimentally obtained modal model on the modal basis of the substructure to accurately estimate the modal parameters of the built-up system. Cuppens et. al [12] provided two methods of dynamic FRF compensation and compensation by residual modes. Based on reconstruction of the interface forces acting between the unknown subsystem and its neighbor, Sjövall and Abrahamsson [13] presented a theoretical method regarding frequency domain load identification. Voormeeren et. al [14] presented a method to quantify the uncertainty of the coupled system's FRFs based on the uncertainties of the subsystem FRFs. Ryberg and Mir [15] developed an experimental model with forward prediction capabilities for passenger vehicle axle whine performance based on FBS techniques to predict the dynamic behavior of complex structures. D'Ambrogio and Sestieri [16] analyzed the possibility of assembling together different substructures' models using expansion techniques to provide the information on the rotational degrees of freedom as well as appropriate modeling of joints and combining modal models and FE models. Sjövall et. al [17] presented a formulation in terms of the state-space parameterization to represent transfer function constraints. Rodriguez et al. [18] presented damage submatrices method (DSM) that localizes and assesses degradation of stiffness at any structural element in a building. And they presented an approach to expand the condensed stiffness matrix of the damaged structure to global coordinates and to identify damage. Ozgen and Kim [19] developed the analytical methods to expand the experimental damping matrix to the size of the analytical model.

This study presents the mathematical form of synthesized and decoupled FRF matrix of substructures utilizing compatibility conditions from the constrained static and dynamic equations. Frequency dependent and time dependent constraint conditions are handled using static and dynamic approaches of constrained systems, respectively. The methods belong to the dual domain method that the interface degrees of freedom of each substructure are retained. It is demonstrated that the proposed methods can simply and explicitly update the FRF matrix and utilize in synthesizing and decoupling of subsystems. Numerical applications evaluate the validity of the proposed methods.

2. FRF based dynamic equation

The response of a dynamic system can be restricted by some kinds of constraints such as prescribed response data or other geometric constraint conditions. The existence of such

constraints leads to the change in its initial response without them. The constrained dynamic response in the frequency-domain is obtained by transforming the initial dynamic equation and the constraints in the time-domain. The following section introduces the constrained dynamic equation in the frequency-domain depending on frequency dependent and time dependent constraint conditions.

2.1 Determination of FRF matrix for constrained dynamic system

This section derives the updated FRF matrix of the constrained dynamic system subjected to frequency dependent and time dependent constraints.

(1) Update of FRF matrix for constrained dynamic system subjected to frequency dependent constraints.

The dynamic response of a discrete system of *n* degrees of freedom with viscous damping is described by ordinary differential equation:

$$\mathbf{M}\ddot{\hat{\mathbf{u}}} + \mathbf{C}\dot{\hat{\mathbf{u}}} + \mathbf{K}\hat{\mathbf{u}} = \mathbf{f} \tag{1}$$

where **M**, **K** and **C** are, respectively, the mass, stiffness and viscous damping matrices; $\hat{\mathbf{u}}$ and **f** denote the response and force vectors corresponding to full degrees of freedom. And the viscous damping assumes the Rayleigh damping.

Transforming Eqn. (1) in the time-domain into the one in the frequency-domain by using $\hat{\mathbf{u}} = \hat{\mathbf{U}}e^{i\omega t}$ and $\mathbf{f} = \mathbf{F}e^{i\omega t}$, it can be rewritten as:

$$\left[-\omega^2\mathbf{M} + i\omega\mathbf{C} + \mathbf{K}\right]\hat{\mathbf{U}}(\omega) = \mathbf{F}(\omega) \tag{2}$$

where $\hat{\mathbf{U}}(\omega)$ and $\mathbf{F}(\omega)$ are the Fourier transform of the response $\hat{\mathbf{u}}(t)$ and force $\mathbf{f}(t)$ for the finite element model. From Eqn. (2), the dynamic stiffness matrix $\hat{\mathbf{D}}(\omega)$ is defined and its inverse the FRF matrix $\hat{\mathbf{H}}$:

$$\hat{\mathbf{D}}(\omega) \equiv -\omega^2\mathbf{M} + i\omega\mathbf{C} + \mathbf{K} \tag{3a}$$

$$\hat{\mathbf{H}}(\omega) = \hat{\mathbf{D}}^{-1}(\omega) = \left[-\omega^2\mathbf{M} + i\omega\mathbf{C} + \mathbf{K}\right]^{-1} \tag{3b}$$

where $\hat{\mathbf{H}}$ and $\hat{\mathbf{D}}$ are analytical FRF and dynamic stiffness matrices, respectively. The dynamic stiffness matrix is a positive definite symmetric matrix because it is expressed by the consistent mass matrix, stiffness matrix and damping matrix.

It is not easy to measure FRF matrix corresponding to full degrees of freedom of the system. Assuming that the system is defected and its displacements at several positions are measured in the frequency-domain or time-domain, the FRF matrix in Eqn. (3b) should be corrected. The measured displacements at *m* positions can be written by:

$$\mathbf{A}\mathbf{U}(\omega) = \mathbf{H}_m(\omega)\mathbf{F}(\omega) \tag{4}$$

where **A** is an $m \times n$ Boolean matrix to define the measurement locations and $\mathbf{H}_m$ denotes an $m \times n$ FRF matrix to be measured, and $\mathbf{U}(\omega)$ indicates the actual displacement vector of the damaged system. And *m* represents the number of impulse force input to act on the system.

The updated dynamic stiffness matrix or FRF matrix must explain the response gap between the initial and actual systems. The response should be described by the constrained static equation because the measured data of Eqn. (4) are not changed with time *t*. Based on the constrained static approach [20], the displacement gap $\delta\mathbf{U}(\omega)$ can be obtained as:

$$\delta\mathbf{U}(\omega) = (\delta\mathbf{H})\mathbf{F} \tag{5}$$

where:

$$\delta\mathbf{H} = \hat{\mathbf{H}}^{1/2}\left(\mathbf{A}\hat{\mathbf{H}}^{1/2}\right)^{+}\left(\mathbf{H}_m - \mathbf{A}\hat{\mathbf{H}}\right) \tag{6}$$

where the superscript '+' is the Moore-Penrose inverse. Thus, the updated expression of FRF

matrix can be written as:

$$\mathbf{H} = \hat{\mathbf{H}} + \delta\mathbf{H} \tag{7}$$

The FRF matrix of Eqn. (7) explains the dynamic characteristics of the full degrees of freedom for the defected system. Premultiplying both sides of Eqn. (6) by $\hat{\mathbf{H}}^{-1}$, it leads to the constraint forces in the frequency-domain expressed by:

$$\mathbf{F}^{c}(\omega) = \hat{\mathbf{H}}^{-1/2}\left(\mathbf{A}\hat{\mathbf{H}}^{1/2}\right)^{+}\left(\mathbf{H}_{m} - \mathbf{A}\hat{\mathbf{H}}\right) \tag{8}$$

The constraint forces represent the additional forces required to obtain the measured or prescribed displacements. An application to utilize the derived equation is illustrated in the following example.

Example 1)

This example considers the update of the FRF matrix of a dynamic system of four degrees of freedom based on measured FRF data of modified dynamic system (Fig. 1). Initial parameter matrices of the system were established as:

$$\mathbf{K} = \begin{bmatrix} 1.5 & -0.5 & 0 & 0 \\ -0.5 & 1.5 & -1 & 0 \\ 0 & -1 & 2 & -1 \\ 0 & 0 & -1 & 1 \end{bmatrix} \times 10^{5}\,\text{N/m}, \quad \mathbf{M} = \begin{bmatrix} 50 & 0 & 0 & 0 \\ 0 & 100 & 0 & 0 \\ 0 & 0 & 100 & 0 \\ 0 & 0 & 0 & 50 \end{bmatrix} \text{kg},$$

$$\mathbf{C} = \begin{bmatrix} 0.15 & -0.1 & 0 & 0 \\ -0.1 & 0.2 & -0.1 & 0 \\ 0 & -0.1 & 0.2 & -0.1 \\ 0 & 0 & -0.1 & 0.1 \end{bmatrix} \text{N}\cdot\text{sec/m}$$

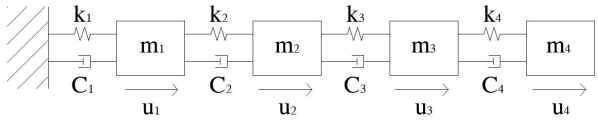

Fig. 1. A dynamic system of four degrees of freedom

Assume that the stiffness k_2 was replaced by $2k_2$ and the FRFs at the second and fourth mass points were experimentally measured to update the parameter matrices. The FRFs corresponding to the two positions were measured as:

$$\mathbf{H}_{m} = \begin{bmatrix} H_{2,1} & H_{2,2} & H_{2,3} & H_{2,4} \\ H_{4,1} & H_{4,2} & H_{4,3} & H_{4,4} \end{bmatrix}$$

where H_{ij} denotes the displacement response measured at location *i* due to the unit force input at location *j*.

The dynamic equation of corrected system needs to modify the initial dynamic equation for satisfying the measured FRFs at the actual state. This numerical application begins with the dynamic system of noise-free FRF data in the range of $0.01-20\text{Hz}$. Figure 2 compares the magnitude of the diagonal components, $H_{i,i}(i = 1,2,3,4)$ in the actual and calculated FRF matrix of the model where the actual and calculated plots indicate the ones calculated from the complete and incomplete measurements, respectively. It is observed that the shapes of both

curves are very similar and the resonance frequencies are rarely changed except $H_{1,1}$. The calculated FRF curves corresponding to measured positions, $H_{2,2}$ and $H_{4,4}$ exactly match with the actual ones and satisfy the constraint conditions of measured FRFs. And the plots exhibit that the little difference in FRF curves of $H_{1,1}$ and $H_{3,3}$ is caused by the incomplete measurements and the discrepancy of FRF curve at mass position 1, $H_{1,1}$ comes from the direct influence on the change in the stiffness k_2. Thus, it is expected that the increase in the number of measurements will result in more exact results and the derived equation will properly describe the dynamic response of the corrected system.

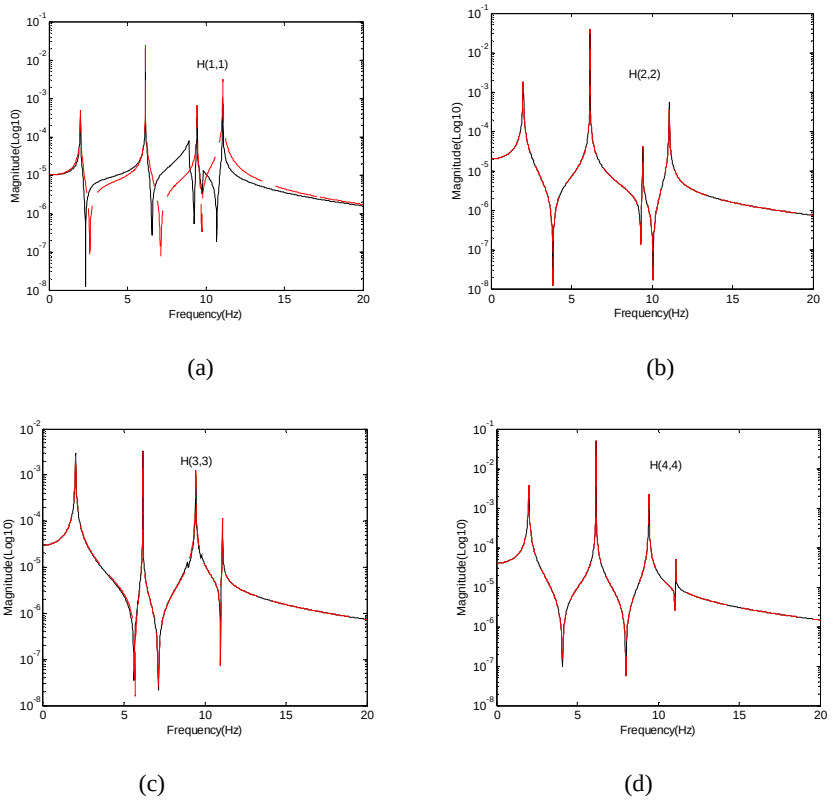

Fig. 2. Spatial plot of the FRF matrix: (a) $H_{1,1}$, (b) $H_{2,2}$, (c) $H_{3,3}$, (d) $H_{4,4}$

The solid line indicates the calculated FRF curve and the dashed line indicates the actual FRF curve.

(2) Update of FRF matrix for constrained dynamic system subjected to time dependent constraints.

From the dynamic equation of motion for unconstrained system of Eqn. (1), its acceleration vector $\mathbf{a}\left(\hat{\mathbf{u}},\dot{\hat{\mathbf{u}}},t\right)$ can be written as:

$$\mathbf{a}=-\mathbf{M}^{-1}\left(\mathbf{C}\dot{\hat{\mathbf{u}}}+\mathbf{K}\hat{\mathbf{u}}-\mathbf{f}\left(t\right)\right) \tag{9}$$

Let us assume that the system is constrained by l $(l<n)$ relations in the time-domain expressed as:

$$\hat{\mathbf{A}}\left(\mathbf{u},\dot{\mathbf{u}},t\right)\ddot{\mathbf{u}}=\hat{\mathbf{b}}\left(\mathbf{u},\dot{\mathbf{u}},t\right) \tag{10}$$

where $\hat{\mathbf{A}}$ is an $l \times n$ matrix, $\mathbf{u}$, $\dot{\mathbf{u}}$ and $\ddot{\mathbf{u}}$ denote the actual displacement, velocity and acceleration vectors, respectively. And l denotes the number of acceleration measurement locations. It is known that the dynamic response of constrained system must satisfy the constraint equations at all times. Utilizing the Moore-Penrose inverse based on the Gauss principle with Eqns. (9) and (10), it can be derived by:

$$\ddot{\mathbf{u}} = \mathbf{a} + \mathbf{M}^{-1/2}\left(\hat{\mathbf{A}}\mathbf{M}^{-1/2}\right)^{+}\left(\hat{\mathbf{b}} - \hat{\mathbf{A}}\mathbf{a}\right) \tag{11}$$

This result represents the dynamic equation of motion for constrained dynamic systems provided by Udwadia and Kalaba [21].

Substituting Eqn. (9) of the acceleration vector at unconstrained state into Eqn. (11) and arranging the result, it can be written in the time-domain as:

$$\mathbf{M}\ddot{\mathbf{u}} + \mathbf{C}^{*}\dot{\mathbf{u}} + \mathbf{K}^{*}\mathbf{u} = \boldsymbol{\alpha}\mathbf{F} + \boldsymbol{\beta} \tag{12}$$

where $\mathbf{C}^{*} = \boldsymbol{\alpha}\mathbf{C}$, $\mathbf{K}^{*} = \boldsymbol{\alpha}\mathbf{K}$, $\boldsymbol{\alpha} = \mathbf{I} - \mathbf{M}^{1/2}\left(\hat{\mathbf{A}}\mathbf{M}^{-1/2}\right)^{+}\hat{\mathbf{A}}\mathbf{M}^{-1}$ and $\boldsymbol{\beta} = \mathbf{M}^{1/2}\left(\hat{\mathbf{A}}\mathbf{M}^{-1/2}\right)^{+}\hat{\mathbf{b}}$.

Transforming the constraint equations of Eqn. (9) into the frequency-domain they can be written as:

$$\mathbf{A}(\omega)\mathbf{U}(\omega) = \mathbf{b}(\omega) \tag{13}$$

where $\mathbf{U}(\omega)$ indicates actual displacement vector in the frequency-domain. And the dynamic equation for constrained systems of Eqn. (12) should be transformed by using $\mathbf{u} = \mathbf{U}e^{i\omega t}$ and $\mathbf{f} = \mathbf{F}e^{i\omega t}$ with Eqn. (13). The ultimate dynamic equation in the frequency-domain can be written as:

$$\mathbf{U}(\omega) = \mathbf{H}^{*}\mathbf{F} + \boldsymbol{\beta} \tag{14}$$

where $\mathbf{H}^{*}$ denotes the $n \times n$ updated FRF matrix of the damaged system,

$$\mathbf{H}^{*} = \left(-\omega^2\mathbf{M} + i\omega\mathbf{C}^{*} + \mathbf{K}^{*}\right)^{-1}\boldsymbol{\alpha}, \quad \boldsymbol{\beta} = \mathbf{M}^{1/2}\left(\mathbf{A}\mathbf{M}^{-1/2}\right)^{+}\mathbf{b}$$

$$\mathbf{C}^{*} = \boldsymbol{\alpha}\mathbf{C}, \quad \mathbf{K}^{*} = \boldsymbol{\alpha}\mathbf{K}, \quad \boldsymbol{\alpha} = \mathbf{I} - \mathbf{M}^{1/2}\left(\mathbf{A}\mathbf{M}^{-1/2}\right)^{+}\mathbf{A}\mathbf{M}^{-1} \tag{15}$$

Given by such constraints as compatibility conditions they lead to:

$$\mathbf{U}(\omega) = \mathbf{H}^{*}\mathbf{F} \tag{16}$$

because the right-hand side of Eqn. (13) should be zero. It is observed that the constrained FRF matrix can be directly and explicitly expressed.

2.2 FBS

The analysis of a huge structure to be composed of r substructures requires sometimes tedious and expensive time. The analysis can be performed by partitioning the entire structure into several substructures and synthesizing them using compatibility conditions between adjacent substructures.

Let us consider the entire structure of r substructures as illustrated in Fig. 3. The dynamic response vector is divided into the internal and boundary regions that are expressed by the superscripts i and b in response vector. The subscripts represent the adjacent substructures to be interconnected. For example, $\hat{\mathbf{u}}^{b}_{j,j+1}(t)$ indicates the response vector at the boundary region between two substructures j and j+1, and $\hat{\mathbf{u}}^{i}_{j}(t)$ the response vector in the internal region of the substructure j.

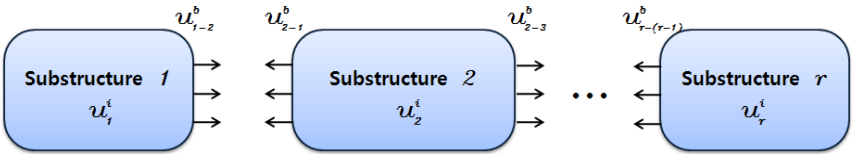

Fig. 3. Substructuring of a huge structure

The dynamic equations of r substructures in the time-domain can be written in the form of Eqn. (1). The compatibility condition between adjacent substructures for structural synthesis must be satisfied while synthesizing the subsystems. The actual compatibility conditions between two subsystems j and $j+1$ are expressed by:

$$\mathbf{u}^b_{j,j+1}(t) = \mathbf{u}^b_{j+1,j}(t) \tag{17}$$

Utilizing the compatibility conditions such as Eqn. (17) into all r substructures and transforming them in the frequency-domain, they can be written by:

$$\mathbf{AU}(\omega) = 0 \tag{18}$$

where $\mathbf{U} = \left[\mathbf{U}_1^T \quad \mathbf{U}_2^T \quad \cdots \quad \mathbf{U}_r^T\right]^T$ and the matrix **A** denotes a Boolean matrix to represent the interfacial nodes of adjacent substructures. Utilizing the unconstrained equation of motion and Eqn. (18) into Eqn. (16) and arranging the result, we obtain the FRF matrix of the synthesized entire system. The following example handles the synthesis of the substructures.

Example 2)

This application considers the synthesis of three subsystems shown in Fig. 4. The subsystems 1, 2 and 3 have 4, 6 and 5 degrees of freedom, respectively, and the entire system has 9 DOFs along with 6 compatibility conditions. The subsystems 1 and 2, and 2 and 3 are interconnected at three nodal points, respectively. The FRF matrix of each subsystem can be established by the mechanical properties of:

$k_1 = 4000\text{N/m}, \quad k_2 = 12000\text{N/m}, \quad k_3 = 8000\text{N/m}, \quad k_4 = 7000\text{N/m}, \quad k_5 = 9000\text{N/m},$

$k_6 = 5000\text{N/m}, \quad k_7 = 6000\text{N/m}, \quad k_8 = 7000\text{N/m}, \quad k_9 = 9000\text{N/m}, \quad k_{10} = 11000\text{N/m},$

$k_{11} = 3000\text{N/m}, \quad k_{12} = 6000\text{N/m}, \quad k_{13} = 5000\text{N/m}, \quad k_{14} = 8000\text{N/m},$

$m_1 = 15\text{kg}, \quad m_2 = 8\text{kg}, \quad m_3 = 10\text{kg}, \quad m_4 = 9\text{kg}, \quad m_5 = 12\text{kg}, \quad m_6 = 13\text{kg}, \quad m_7 = 9\text{kg}, \quad m_8 = 13\text{kg},$

$m_9 = 17\text{kg}, \quad \mathbf{C} = 0.0001\mathbf{K},$

where **C** and **K** are damping and stiffness matrices, respectively. The damping matrix is proportional to the stiffness matrix.

The subsystems were divided at mass locations indicated in the figure and the constants α_i and $\beta_i (i = 1,2,3)$ denote the fraction of the divided mass. The mass fractions were selected as $\alpha_1 = \alpha_2 = \alpha_3 = 0.9$ and $\beta_1 = \beta_2 = \beta_3 = 0.9$. The compatibility conditions at the interfaces transformed into the frequency-domain are written by:

$U_2(\omega) = U_2'(\omega), \quad U_3(\omega) = U_3'(\omega), \quad U_4(\omega) = U_4'(\omega), \quad U_5(\omega) = U_5'(\omega), \quad U_6(\omega) = U_6'(\omega),$

$U_7(\omega) = U_7'(\omega).$

Inserting the measured FRF matrices of three subsystems and compatibility conditions into Eqn. (16), the FRFs in the frequency range of $0.01 - 40\text{Hz}$ were calculated.

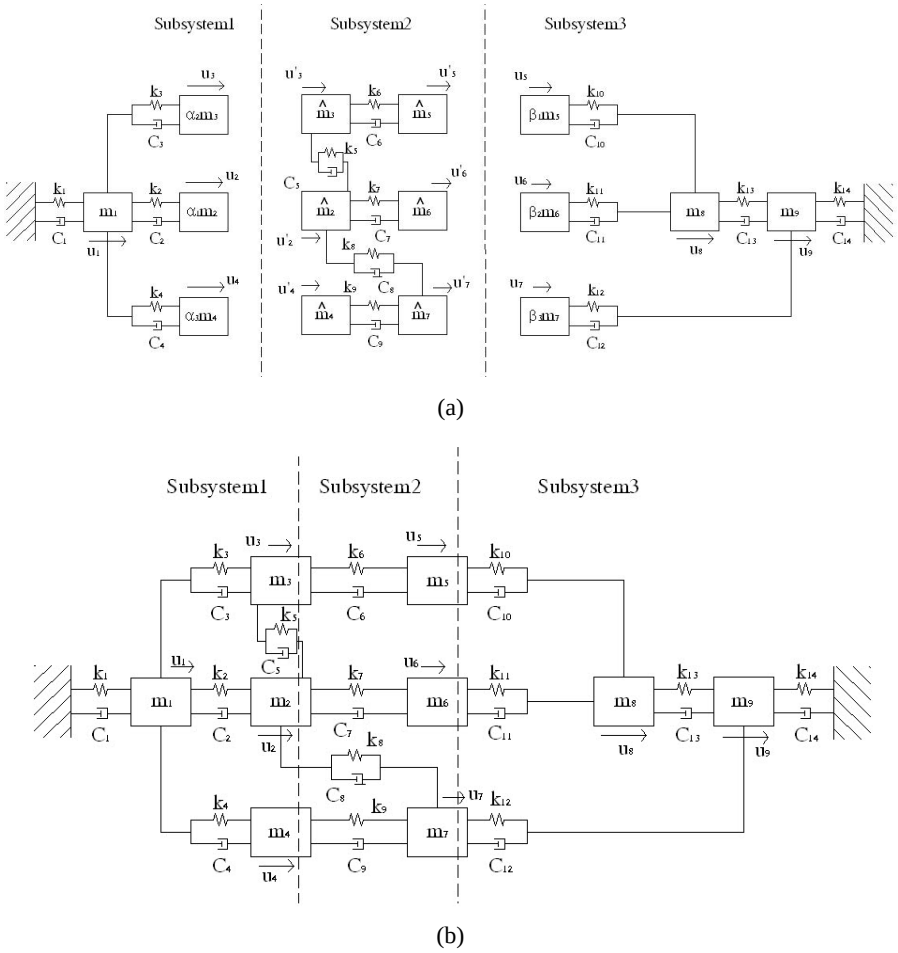

Fig. 4. A dynamic system: (a) partitioned subsystems, (b) an entire system

$$\hat{m}_2 = 01m_2,\ \ \hat{m}_3 = 0.1m_3,\ \ \hat{m}_4 = 0.1m_4,\ \ \hat{m}_5 = 0.1m_5,\ \ \hat{m}_6 = 0.1m_6,\ \ \hat{m}_7 = 0.1m_7$$

The calculated FRF matrix takes a matrix form corresponding to the dual domain. Figure 5 compares the FRF curves of the diagonal components in the FRF matrices of the synthesized system and initial entire system. It is shown that those plots are the same and the derived equation can exactly describe the dynamic responses of the synthesized system in the satisfaction of the compatibility conditions. It indicates that the derived method can exactly and explicitly establish the FRF matrix in synthesizing the substructures based on dual assembly.

2. 3. FBD

The decoupling process follows the converse process of the substructuring. As an application of the decoupling, we can consider the identification problem of a subsystem which cannot be removed or accessed easily. That is, if the dynamic equation of motion for an entire structure E and a substructure B are given, the residual subsystem (E-B) can be extracted from the entire system E in the frequency-domain by removing the dynamic effect of the substructure B in Fig. 6.

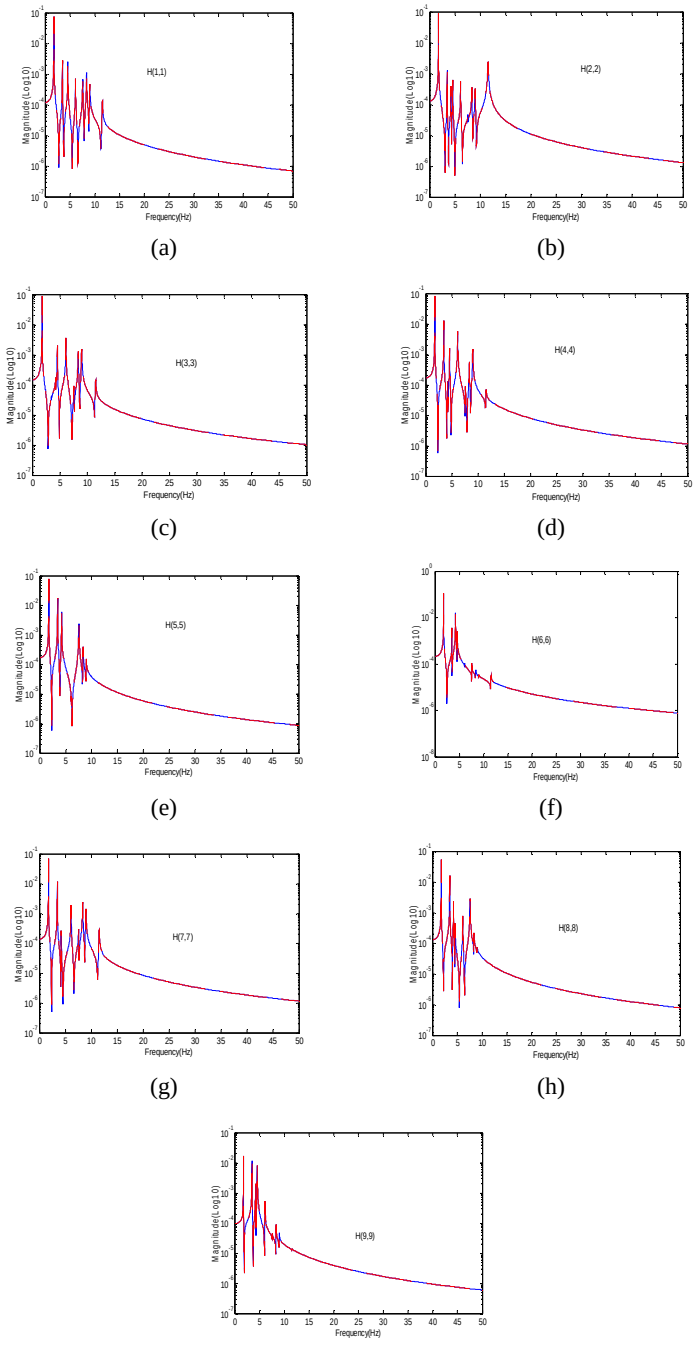

Fig. 5. Spatial plot of the FRF matrix: (a) $H_{1,1}$, (b) $H_{2,2}$, (c) $H_{3,3}$, (d) $H_{4,4}$, (e) $H_{5,5}$, (f) $H_{6,6}$, (g) $H_{7,7}$, (h) $H_{8,8}$, (i) $H_{9,9}$. The solid line indicates the actual FRF curve and the dotted line indicates the calculated FRF curve

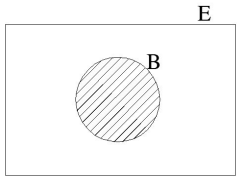

Fig. 6. Decoupling from an entire system

Let us consider an entire system E to be composed of *s* substructures in Fig. 7. Assuming that the dynamic characteristics of the entire structure and the *j*-th substructure to be removed are known, this work estimates the dynamic characteristics of the residual substructure. The compatibility conditions between the residual system and the deleted subsystem *j* can be written by:

$$\mathbf{A}^{*}\begin{bmatrix}\mathbf{u}(t)\\ \mathbf{u}_{j}(t)\end{bmatrix}=\mathbf{0} \tag{19}$$

where $\mathbf{A}^{*}$ denotes a Boolean matrix to define the interfacial positions between the entire system and the subsystem *j*.

Expressing the dynamic equations of the entire system and Eqn. (19) into Eqn. (11) and changing the (+) sign of the term to represent displacement variation to the sign (-), they can be written by:

$$\mathbf{M}\ddot{\mathbf{u}}+\mathbf{C}^{*}\dot{\mathbf{u}}+\mathbf{K}^{*}\mathbf{u}=\xi\mathbf{F} \tag{20}$$

where $\mathbf{C}^{*}=\xi\mathbf{C}$, $\mathbf{K}^{*}=\xi\mathbf{K}$ and $\xi=\mathbf{I}+\mathbf{M}^{1/2}\left(\mathbf{A}^{*}\mathbf{M}^{-1/2}\right)^{+}\mathbf{A}^{*}\mathbf{M}^{-1}$.

Equations (19) and (20) should be transformed by using $\mathbf{u}=\mathbf{U}e^{i\omega t}$ and $\mathbf{f}=\mathbf{F}e^{i\omega t}$. The ultimate dynamic equation in the frequency-domain can be written as:

$$\mathbf{U}(\omega)=\mathbf{H}^{*}\mathbf{F} \tag{21}$$

$$\mathbf{A}\mathbf{U}(\omega)=\mathbf{0} \tag{22}$$

where $\mathbf{H}^{*}$ denotes the $n\times n$ updated FRF matrix of the residual system based on dual domain decomposition written by:

$$\mathbf{H}^{*}=\left(-\omega^{2}\mathbf{M}+i\omega\mathbf{C}^{*}+\mathbf{K}^{*}\right)^{-1}\xi \tag{23}$$

It is observed that the constrained FRF matrix can be directly and explicitly expressed. The FRF matrix of Eqn. (23) describes the dynamic characteristics of the residual system to delete the *j*-th subsystem. It is demonstrated that the FRF matrix for the residual system also takes an explicit form.

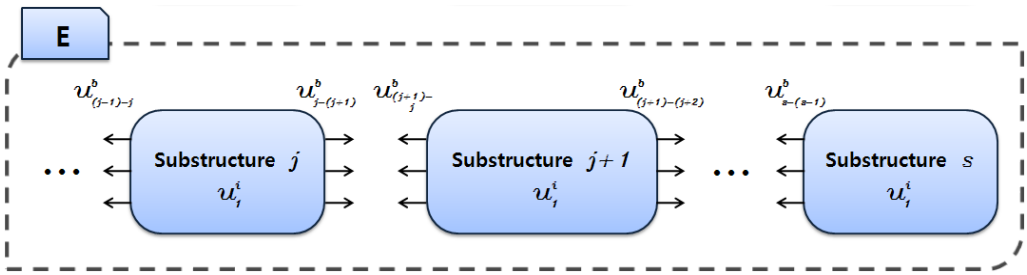

Fig. 7. Decoupling of substructures

Example 3)

This example considers the establishment of the FRF curve of the residual system to remove a part of the subsystem 2 from the entire system in Fig. 8. Providing all information on the entire system as well as the removed part of subsystem 2, we can estimate the FRF matrix of the residual system. Inserting the dynamic equations of the entire system and the part of subsystem 2, and the compatibility conditions into Eqn. (22), the FRF curves corresponding to the residual system are predicted.

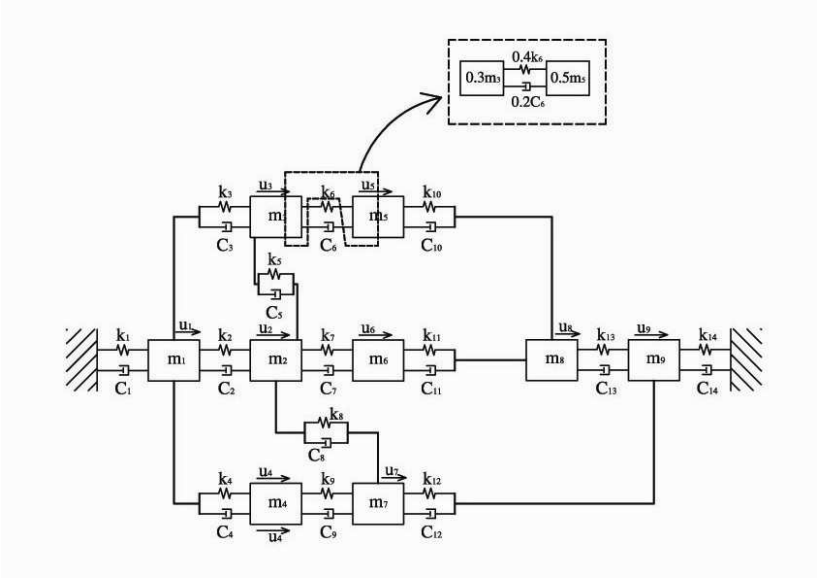

Fig. 8. An entire system and removed part of the subsystem 2

Figure 9 compares the FRF curves of the residual system after decoupling and the entire system. The plots exhibit the influence due to the removal of the subsystem. It is found that both FRF curves of the entire system and residual system exhibit different shapes in the low frequency range corresponding to resonance and anti-resonance, and are very similar after the frequency range. The derived equation can properly describe the residual responses by simply substituting the dynamic equations of the entire system as well as the removed subsystem and the compatibility conditions into the governing equation of Eqn. (22)

3. Conclusions

This study provided analytical formulations to update the full set of FRF matrix from the dynamic equation of initial system and frequency or time dependent constraints. It was demonstrated that the proposed methods can be utilized in synthesizing subsystems and decoupling subsystems from an entire system based on dual domain components. The validity of the proposed method was illustrated and analyzed through numerical applications.

Acknowledgement

This Research was supported by the Chung-Ang University Research Scholarship Grants in 2008.

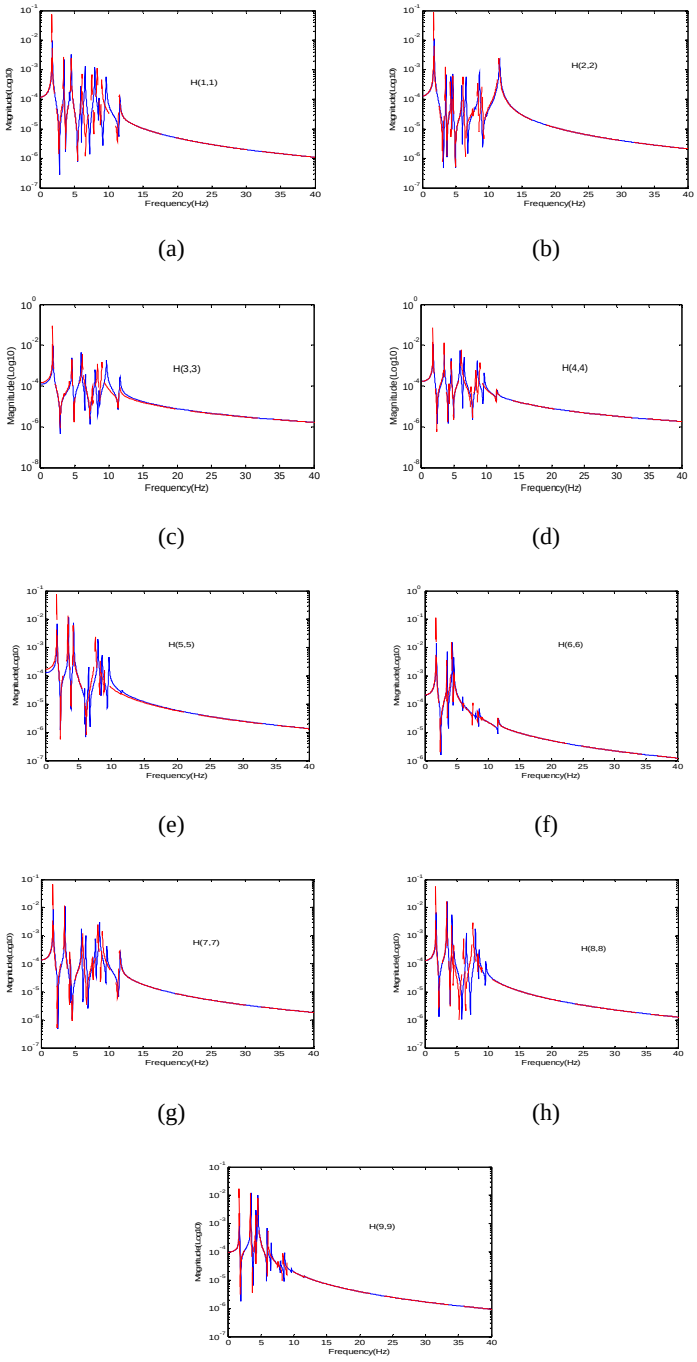

(a) (b) (c) (d) (e) (f) (g) (h) (i)

Fig. 9. Spatial plot of the FRF matrix: (a) $H_{1,1}$, (b) $H_{2,2}$, (c) $H_{3,3}$, (d) $H_{4,4}$, (e) $H_{5,5}$, (f) $H_{6,6}$, (g) $H_{7,7}$, (h) $H_{8,8}$, (i) $H_{9,9}$. The solid line indicates the residual system calculated FRF curve and the dashed line indicates the actual FRF curve

References

[1] Hurty W. C. Vibrations of structural systems by component mode synthesis. Journal of Engineering Mechanics 1960, 86: 51-69.

[2] Hurty W. C. Dynamic analysis of structural systems using component modes. AIAA Journal 1965, 3: 678-685.

[3] Craig Jr. R. R., Bampton M. C. C. Coupling of substructures for dynamic analysis. AIAA Journal 1968, 6: 1313-1319.

[4] Craig Jr. R. R. A review of time-domain and frequency domain component-mode synthesis method. International Journal of Analytical and Experimental Modal Analysis 1987, 2: 59-72.

[5] Craig Jr. R. R., Ni Z. Component-mode synthesis for model order reduction of nonclassically damped systems. AIAA Journal of Guidance, Control, and Dynamics 1989, 12: 577-84.

[6] MacNeal R. H. A hybrid method of component mode synthesis. Computers and Structures 1971, 1: 581-601.

[7] Rubin S. Improved component-mode representation for structural dynamic analysis. AIAA Journal 1975, 13: 995-1006.

[8] De Lima A. M. G., Rade D. A., Lépore Neto F. P. An efficient modeling methodology of structural systems containing viscoelastic dampers based on frequency response function substructuring. Mechanical Systems and Signal Processing 2009, 23: 1272-1281.

[9] Klerk D., Rixen D. J., Voormeeren S. N. General framework for dynamic substructuring: History, review, and classification of techniques. AIAA Journal 2008, 46: 1169-1181.

[10] D'Ambrogio W., Fregolent A. The role of interface DoFs in decoupling of substructures based on the dual domain decomposition. Mechanical Systems and Signal Processing 2010, 24: 2035-2048.

[11] Allen M. S., Mayes R. N., Bergman E. J. Experimental modal substructuring to couple and uncouple substructures with flexible fixtures and multi-point connections. Journal of Sound and Vibration 2010, 329: 4891-4906.

[12] Cuppens K., Sas P., Hermans L. Evaluation of the FRF based substructuring and modal synthesis technique applied to vehicle FE data, International Conference on Noise and Vibration Engineering 2000, 25: 1143-1150.

[13] Sjövall P., Abrahamsson T. Structural system identification from coupled system test data. Mechanical Systems and Signal Processing 2008, 22: 15-33.

[14] Voormeeren S. N., Klerk D., Rixen D. J. Uncertainty quantification in experimental frequency based substructuring. Mechanical Systems and Signal Processing 2010, 106-118.

[15] Ryberg D., Mir H. Development of an Experimental FRF-Based Substructuring Model to Forward Predict the Effects of Beam Axle Design Modifications on Passenger Vehicle Axle Whine. SAE 2007 Noise and Vibration Conference and Exhibition.

[16] D'Ambrogio W., Sestieri A. A unified approach to substructuring and structural modification problems. Shock and Vibration 2004, 11: 295-309.

[17] Sjövall P., McKelvey T., Abrahamsson T. Constrained state-space system identification with application to structural dynamics. Automatica 2006, 42: 1539-1546.

[18] Rodriguez R., Escobar J. A., Gomez R. Damage location and assessment along structural elements using damage submatrices. Engineering Structures 2009, 31: 475-486.

[19] Ozen G. O., Kim J. H. Direct identification and expansion of damping matrix for experimental-analytical hybrid modeling. Journal of Sound and Vibration 2007, 308: 348-372.

[20] Eun H. C., Lee E. T., Chung H. S. On the static analysis of constrained structural systems. Canadian Journal of Civil Engineering 2004, 31: 1119-1122.

[21] Udwadia F. E., Kalaba R. E. A New Perspective on Constrained Motion. Proceedings of the Royal Society of London 1992, 439: 407-410.